

In Vitro Phase I Metabolism of *cis*-Zearalenone

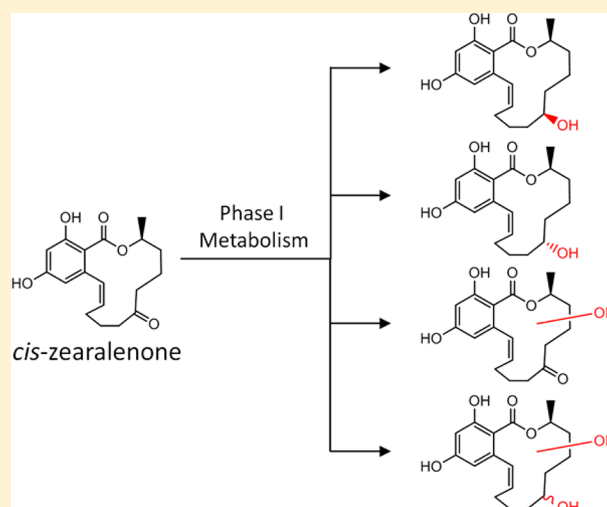
Sarah S. Drzymala,^{*,†} Antje J. Herrmann,[†] Ronald Maul,^{†,‡} Dietmar Pfeifer,[†] Leif-Alexander Garbe,[§] and Matthias Koch[†]

[†]Department of Analytical Chemistry; Reference Materials, Federal Institute for Materials Research and Testing (BAM), Richard-Willstaetter-Strasse 11, 12489 Berlin, Germany

[‡]Department of Quality, Leibniz-Institute of Vegetable and Ornamental Crops (IGZ), Theodor-Echtermeyer-Weg 1, 14979 Großbeeren, Germany

[§]Department of Biotechnology, Institute of Bioanalytics, Technische Universität Berlin, 13353 Berlin, Germany

ABSTRACT: The present study investigates the *in vitro* phase I metabolism of *cis*-zearalenone (*cis*-ZEN) in rat liver microsomes and human liver microsomes. *cis*-ZEN is an often ignored isomer of the *trans*-configured *Fusarium* mycotoxin zearalenone (*trans*-ZEN). Upon the influence of (UV-) light, *trans*-ZEN isomerizes to *cis*-ZEN. Therefore, *cis*-ZEN is also present in food and feed. The aim of our study was to evaluate the *in vitro* phase I metabolism of *cis*-ZEN in comparison to that of *trans*-ZEN. As a result, an extensive metabolization of *cis*-ZEN is observed for rat and human liver microsomes as analyzed by HPLC-MS/MS and high-resolution MS. Kinetic investigations based on the substrate depletion approach showed no significant difference in rate constants and half-lives for *cis*- and *trans*-ZEN in rat microsomes. In contrast, *cis*-ZEN was depleted about 1.4-fold faster than *trans*-ZEN in human microsomes. The metabolite pattern of *cis*-ZEN revealed a total of 10 phase I metabolites. Its reduction products, α - and β -*cis*-zearalenol (α - and β -*cis*-ZEL), were found as metabolites in both species, with α -*cis*-ZEL being a major metabolite in rat liver microsomes. Both compounds were identified by co-chromatography with synthesized authentic standards. A further major metabolite in rat microsomes was monohydroxylated *cis*-ZEN. In human microsomes, monohydroxylated *cis*-ZEN is the single dominant peak of the metabolite profile. Our study discloses three metabolic pathways for *cis*-ZEN: reduction of the keto-group, monohydroxylation, and a combination of both. Because these routes have been reported for *trans*-ZEN, we conclude that the phase I metabolism of *cis*-ZEN is essentially similar to that of its *trans* isomer. As *trans*-ZEN is prone to metabolic activation, leading to the formation of more estrogenic metabolites, the novel metabolites of *cis*-ZEN reported in this study, in particular α -*cis*-ZEL, might also show higher estrogenicity.



INTRODUCTION

trans-Zearalenone (*trans*-ZEN) is an estrogenic mycotoxin that contaminates food and feed worldwide. It is produced by various molds of the *Fusarium* genus, which can infest cereal crops including wheat, rye, oats, soybeans, rice, and maize. Humans and animals are exposed to *trans*-ZEN by ingestion of contaminated food and feed. The spatial structure of *trans*-ZEN enables binding to the mammalian estrogen receptor, thus causing reproductive disorders in numerous animal species and possibly in humans.¹ Thus, maximum levels have been established for this fungal toxin in the European Union (EU) and several countries worldwide.² In the EU, maximum levels range between 20 and 400 $\mu\text{g}/\text{kg}$, depending on the commodity.³

Concerning phase I metabolism, several mammalian *in vitro* and *in vivo* studies have shown that *trans*-ZEN is extensively metabolized via reduction and hydroxylation. Reduction

products were found in various animal species and humans, in particular α - and β -*trans*-zearalenol (α - and β -*trans*-ZEL).^{4–7} The estrogenic activity of α -*trans*-ZEL exceeds that of *trans*-ZEN by approximately a factor of 80, thus linking the toxicity of *trans*-ZEN inevitably to its metabolism.⁸ Several monohydroxylated metabolites were discovered in rat and human *in vitro* assays, including one monohydroxylated ZEN discovered in rat urine *in vivo*.^{9–12}

Various studies demonstrated that *trans*-ZEN is subject to phase II metabolism. Conjugation of *trans*-ZEN with glucuronic acid and sulfate proved to be a major metabolic pathway in different animal species and humans *in vitro* as well as *in vivo*.^{13–15} These reports also show that phase I metabolites of *trans*-ZEN are prone to conjugation reactions.

Received: July 31, 2014

Published: September 25, 2014

Although often ignored, ZEN can occur in two configurations. The double bond between C11 and C12 may isomerize from the *trans* to the *cis* configuration (Figure 1).

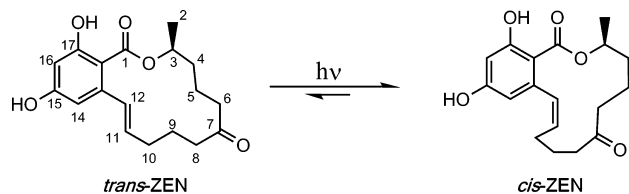


Figure 1. Photoisomerization of ZEN.

Routes of entry into the food chain might arise from the production of *cis*-ZEN by fungi^{16,17} or upon exposure of *trans*-ZEN contaminated foods to (UV-) light, although the detection of *cis*-ZEN in fungi cultures might be a consequence of exposure to daylight, as biosynthetic pathways are generally stereoselective. To date, *cis*-ZEN has been detected in different commodities like ground maize, sugar beets, and edible oils as well as in wet ground maize intended for animal feeding.^{18–20}

Despite the evidence of *cis*-ZEN occurrence in food and feed, its metabolism has never been investigated. Presumably, the lacking availability of authentic standards and missing adequate analytical methods have hampered a comprehensive investigation of *cis*-ZEN metabolism. In order to address this problem, we recently synthesized *cis*-ZEN and ¹³C-labeled *cis*-ZEN.^{19,21} Applying these standards, the aim of the present work is to investigate the *in vitro* depletion kinetics of *cis*-ZEN and to identify novel metabolites in rat and human liver microsomes.

MATERIALS AND METHODS

Terms and Definitions. Throughout the entire article, the term zearalenone (ZEN) or zearalenol (ZEL) refers to both *cis* and *trans* isomers. When a certain isomer is considered, it will be specified by either *trans* or *cis*.

Chemical Reagents. *trans*-ZEN (white powder, purity 99.8%) was purchased from AppliChem GmbH (Darmstadt, Germany). Zearalanone (purity 98.0%), α -*trans*-ZEL (no purity given), and β -*trans*-ZEL (no purity given) were obtained from Sigma-Aldrich (Steinheim, Germany). NADPH tetrasodium salt was obtained from AppliChem GmbH (Darmstadt, Germany). MgCl₂ was purchased from Avantor Performance Materials (Center Valley, PA, USA). KH₂PO₄ was derived from Merck (Darmstadt, Germany) and K₂HPO₄ from Carl

Roth (Karlsruhe, Germany). All standard chemicals were of p.a. grade, and all solvents, HPLC grade.

Microsomal Source. Human and rat liver microsomes were purchased from BioreclamationIVT (Baltimore, MD, USA). Rat liver microsomes (RLM) were prepared from Sprague–Dawley female rats. Human liver microsomes (HLM) were derived from a mixed gender pool of 50 donors. The total protein content, P450 concentrations, and specific activities of different P450 isoforms were assumed as provided by the manufacturer. Regarding RLM, the protein concentration was 23.7 mg/mL, and the total P450 concentration, 0.483 nmol/mg. For HLM, the protein concentration was 20.0 mg/mL, and the total P450 concentration, 0.411 nmol/mg.

Preparation of Native and ¹³C-Labeled *cis*-Zearalenone.

Native *cis*-ZEN was generated photochemically from *trans*-ZEN by a procedure reported earlier.¹⁹ In summary, native *trans*-ZEN is dissolved in ethyl acetate and irradiated by UV-light ($\lambda = 350$ nm) for 8 h. The irradiated solution is then subjected to preparative HPLC in order to separate the *trans* from the *cis* isomer and to obtain pure native *cis*-ZEN. U-¹³C₁₈-*cis*-ZEN was synthesized as described earlier following the same procedure as that for the preparation of native *cis*-ZEN.¹⁹ Purities were determined to be >99% for the native as well as the ¹³C-labelled standard, as measured by HPLC-FLD.

Microsomal Incubations. Incubations of ZEN with either RLM or HLM were carried out at 37 °C in a volume of 0.2 mL. For kinetic investigations, a mixture containing 1 μ M ZEN dissolved in DMSO, microsomes (final protein concentration 1 mg/mL), 0.1 mM MgCl₂, and 0.1 M potassium phosphate buffer, pH 7.4, was preincubated for 5 min. The fraction of DMSO in the microsomal incubation volume was not higher than 1%. Reactions were started by adding 6 mM NADPH. At different time points the reaction was quenched by addition of equal volumes of ice-cold acetonitrile containing internal standard. The respective fully ¹³C-labeled ZEN analogues were used for quantification of *cis*- and *trans*-ZEN. After the reaction was stopped, the incubation mixtures were centrifugated in a Eppendorf mini Spin plus centrifuge (Hamburg, Germany) at 11 650g for 5 min. The supernatant was transferred to a HPLC vial and analyzed by HPLC-MS/MS. Negative controls lacked NADPH. Vehicle controls contained NADPH but no substrate. A control containing NADPH and substrate but without microsomes was performed as well. Control incubations were performed in duplicate; all other reactions were performed in triplicate.

In order to calculate depletion kinetics, the peak areas of *cis*- or *trans*-ZEN were determined and normalized to the value obtained at $t = 0$ min. Rate constants k (min⁻¹) were obtained by linear least-squares regression of the term $\ln(A/A_0) = -kt$, where t is the incubation time (min), A is the peak area, and A_0 is the peak area at $t = 0$ min. Half-lives were calculated according to the expression $t_{1/2} = \ln 2/k$, as reported by Obach and colleagues.²²

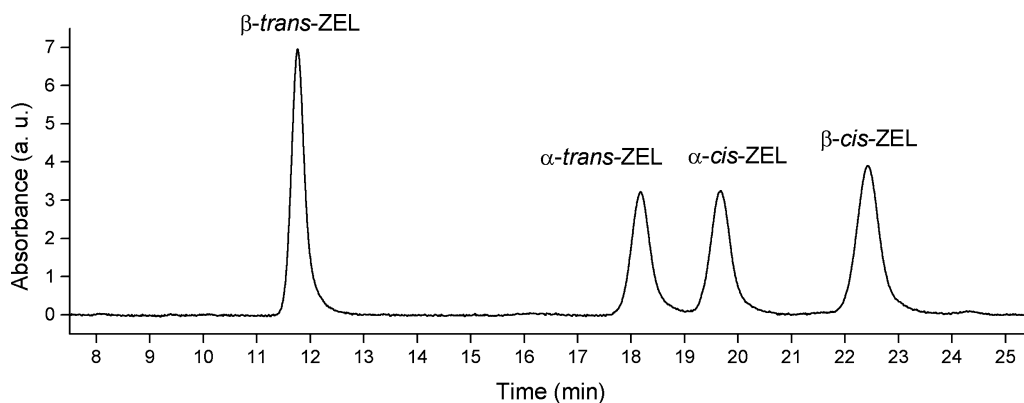


Figure 2. HPLC-DAD ($\lambda = 274$ nm) chromatogram of α -/ β -*trans*-ZEL after UV irradiation for 12 h. The mixture of the four isomers can be well-separated using a C18 column. Retention times differ from the metabolite patterns in Figures 4 and 5 due to the use of a different analytical column and method.

In contrast to the kinetic investigations, 10 μM ZEN were used as the substrate concentration for qualitative analysis to enhance the signal intensity of the formed metabolites. The reaction was run for a time period of 120 min and then stopped by addition of 50 μL ice-cold acetonitrile. Analysis was carried out by high-resolution mass spectrometry (HRMS). Phase I metabolites were identified by comparing chromatograms from vehicle control and negative control incubations to that from incubations in the presence of NADPH. Furthermore, incubations in the presence of NADPH were compared to incubations containing NADPH and substrate but without microsites. All other conditions were as stated for the kinetic investigations.

Metabolite Synthesis: α - and β -cis-Zearalenol. In a series of pretests, standards of α - and β -trans-ZEL were UV-irradiated separately at $\lambda = 350$ nm. Each standard gave rise to one main irradiation product, which was tentatively assigned α - or β -cis-ZEL, depending on the configuration of the educt. The maximum *cis*-ZEL formation was observed after 24 h for α -trans-ZEL and after 48 h for β -trans-ZEL. Irradiation in ethyl acetate yielded the highest *cis*-/*trans*-ZEL ratio (α -ZEL, 3.5; β -ZEL, 3.6) when compared to heptane, acetonitrile, acetone, and methanol, confirming the results of Koppen et al.¹⁹ for ZEN isomerization.

For final synthesis of the *cis*-ZELs, a two step procedure was planned using sodium borohydride reduction of *trans*-ZEN and subsequent UV radiation. Due to the isomerization equilibrium of the *trans*- and *cis*-ZELs after irradiation, a suitable analytical method was developed to separate all four ZEL isomers in one run (Figure 2). The chromatographic system consisted of a SpectraSystem HPLC (Thermo Fisher Scientific, Waltham, MA, USA) including a pump P4000, a degasser SCM 1000F, an autosampler AS3000F, a DAD UV6000LP, and a FLD Surveyor Plus with a Eurospher II 100-3 C18 P column (150 \times 2 mm, 3 μm particle size; Knauer GmbH, Berlin, Germany). A 50 $^{\circ}\text{C}$ oven temperature, an injection volume of 10 μL , a flow rate of 0.4 mL/min, and a runtime of 30 min were employed. Methanol/water 45:55 (v/v) containing 0.1% formic acid was used as isocratic elution solvent. The DAD was set to $\lambda = 274$ nm, and fluorescence detection was done at $\lambda_{\text{Ex}} = 274$ nm and $\lambda_{\text{Em}} = 456$ nm.

Final synthesis of both *cis*-ZEL isomers was carried out with 38 mg of NaBH_4 (1.0 mmol), which was added to a solution of 25 mg of *trans*-ZEN (0.9 mmol) in 10 mL of methanol. After 15 min at room temperature, the reaction was stopped by dropwise addition of acetic acid (25% in water) until no further gas formation could be observed. The completion of the reaction was confirmed by HPLC-FLD (chromatography conditions as stated above). The ratio of α - to β -trans-ZEL was calculated from HPLC-DAD peak area ($\lambda = 274$ nm) as 33:67. The solution was evaporated to dryness, redissolved in ethyl acetate, and split into 10 fractions in clear glass HPLC vials, which were directly exposed to UV light ($\lambda = 350$ nm). The exposure was carried out for 24 h using a universal UV lamp, type TL-900 (CAMAG, Muttenz, Switzerland). The generated *cis* isomers were purified from the *trans* isomers using the chromatographic conditions described above with the HPLC system connected to an automatic fraction collector Foxy Jr. (Teledyne Isco, Lincoln, NE, USA). The purification yielded 5.6 mg (22%) of α -cis-ZEL in a purity > 94% and 7.0 mg of β -cis-ZEL in a purity > 99%. Purities were determined by HPLC-UV analysis at $\lambda = 274$ nm.

The accurate mass of the *cis*-ZELs was determined by HRMS (m/z 319.157 for both) and matches the calculated exact mass for ZEL. Furthermore, the configuration of the double bond C11–C12 was resolved by ^1H NMR. NMR spectra were recorded on a Bruker DMX-400 or a Bruker AVANCE III 500 spectrometer (Bruker Daltonik, Bremen, Germany) in CD_3OD . Proton chemical shifts were referenced to residual native methanol at 3.31 ppm. Complete assignments for proton resonances were performed in accordance to previously published works on α - and β -trans-ZEL.²³

α -trans-ZEL. δ (ppm) 1.16–1.94 (m, 10H, H-4, H-5, H-6, H-8, H-9), 1.39 (d, 3H, $-\text{CH}_3$, $J = 6.1$ Hz), 2.32 (m, 2H, H-10), 3.76 (m, 1H, H-7), 4.96 (m, 1H, H-3), 5.70 (ddd, 1H, H-11, $J = 15.4, 9.9, 4.6$ Hz), 6.22 (d, 1H, H-15, $^4J_{(13,15)} = 2.5$ Hz), 6.37 (d, 1H, H-13, $^4J_{(13,15)} = 2.5$ Hz), 7.12 (d, 1H, H-12, $J_{(12,11)} = 15.4$ Hz).

α -cis-ZEL. δ (ppm) 1.24–1.82 (m, 10H, H-4, H-5, H-6, H-8, H-9), 1.35 (d, 3H, $-\text{CH}_3$, $J = 6.2$ Hz), 2.28 (m, 2H, H-10), 3.75 (m, 1H, H-7), 5.15 (m, 1H, H-3, $J = 6.2$ Hz), 5.57 (ddd, 1H, H-11, $J = 11.5, 11.2, 3.8$ Hz), 6.14 (d, 1H, H-15, $^4J_{(13,15)} = 2.5$ Hz), 6.23 (d, 1H, H-13, $^4J_{(13,15)} = 2.5$ Hz), 6.71 (d, 1H, H-12, $J_{(12,11)} = 11.5$ Hz).

β -trans-ZEL. δ (ppm) 1.29–1.79 (m, 10H, H-4, H-5, H-6, H-8, H-9), 1.34 (d, 3H, $-\text{CH}_3$, $J = 6.2$ Hz), 2.28 (m, 2H, H-10), 3.71 (m, 1H, H-7), 5.12 (m, 1H, H-3, $J = 6.3$ Hz), 5.96 (ddd, 1H, H-11, $J = 15.5, 8.4, 6.0$ Hz), 6.21 (d, 1H, H-15, $^4J_{(13,15)} = 2.5$ Hz), 6.44 (d, 1H, H-13, $^4J_{(13,15)} = 2.5$ Hz), 6.72 (d, 1H, H-12, $J_{(12,11)} = 15.6$ Hz).

β -cis-ZEL. δ (ppm) 1.28–1.69 (m, 10H, H-4, H-5, H-6, H-8, H-9), 1.36 (d, 3H, $-\text{CH}_3$, $J = 6.5$ Hz), 2.17 (m, 2H, H-10), 3.60 (m, 1H, H-7), 5.34 (m, 1H, H-3, $J = 6.5$ Hz), 5.60 (ddd, 1H, H-11, $J = 11.5, 10.1, 5.1$ Hz), 6.14 (d, 1H, H-15, $^4J_{(13,15)} = 2.5$ Hz), 6.22 (d, 1H, H-13, $^4J_{(13,15)} = 2.5$ Hz), 6.72 (d, 1H, H-12, $J_{(12,11)} = 11.5$ Hz).

HPLC-MS Analysis. HPLC-MS/MS. Kinetic experiments were analyzed on an Agilent 1200 series HPLC coupled to an API 4000 QTRAP hybrid mass spectrometer (AB Sciex, Foster City, USA). A Gemini-NX C₁₈ column (150 mm \times 2 mm, 3 μm particle size; Phenomenex, Aschaffenburg, Germany) was used with a flow rate of 0.25 mL/min and an oven temperature of 50 $^{\circ}\text{C}$. The mobile phase consisted of water with 0.1% formic acid (A) and methanol containing 0.1% formic acid (B). A gradient program was used starting at 50% mobile phase B. Within 17 min, B was raised to 60%, followed by an increase to 100% at minute 18. Afterwards, the column was re-equilibrated to starting conditions for 5 min. HPLC-MS/MS runtime was 24 min per sample, and the injection volume was set to 10 μL .

The mass spectrometer was operated in multiple reaction monitoring (MRM) mode with negative electrospray ionization (ESI). For both native ZEN isomers, the monitored transitions were (m/z) 317.1 \rightarrow 131.1 (quantifier) and 317.1 \rightarrow 175.0 (qualifier). For the two internal standards, U- $^{13}\text{C}_{18}$ -ZEN (m/z) 335.2 \rightarrow 140.2 was monitored. *trans*- and *cis*-ZEN were separated by chromatography and assigned via retention times.

The following ion source parameters were used: ion spray voltage, -4000 V; desolvation temperature, 450 $^{\circ}\text{C}$; ion source gas, 1:60; ion source gas, 2:60; curtain gas, 20. The optimized MRM compound-specific parameters were (quantifier/qualifier/internal standard): declustering potential, $-65/-65/-65$ V; entrance potential, $-10/-10/-10$ V; collision energy, $-40/-34/-40$ V; collision cell exit potential, $-9/-6/-9$ V; dwell time, 50/50/50 ms. Data acquisition was done using Analyst 1.6.2 software (AB Sciex, Foster City, CA, USA).

HRMS. Qualitative metabolite profiling and accurate mass based analyses were done on an Agilent 1290 Infinity UPLC coupled to an Agilent 6230 accurate-mass time-of-flight MS. The column oven was set to 50 $^{\circ}\text{C}$. Separation of the metabolites was achieved on an Ascentis Express F5 column (150 mm \times 3 mm, 2.7 μm particle size; Sigma-Aldrich, Steinheim, Germany). The Ascentis F5 column separated *trans*- and *cis*-ZEN as well as the *cis* and *trans* isomers of α - and β -ZEL using water with 0.1% formic acid (A) and methanol containing 0.1% formic acid (B) as solvents in a gradient program at a flow rate of 0.35 mL/min. A linear gradient was applied starting from 50% B to 70% at minute 18. Then, the column was re-equilibrated for 8 min.

For ESI operation, nitrogen was used as the drying gas (350 $^{\circ}\text{C}$, 10 L/min) and nebulizer gas (35 psi). The capillary, skimmer, and octapole RF voltages were set at 3.7 kV, 65 V, and 750 V, respectively. Data was acquired in the negative ionization mode within a range of 75 to 500 m/z . Automatic calibration was enabled by continuous postcolumn infusion of calibrant solution. Data analysis was done using MassHunter 6.0. Determination of the elemental composition of individual metabolites was based on accurate masses, typically better than 10 ppm mass accuracy.

RESULTS

Depletion Kinetics. In the presence of NADPH, *cis*-ZEN is rapidly metabolized by rat liver microsomes (RLM) and human liver microsomes (HLM), which can be seen by the decrease of

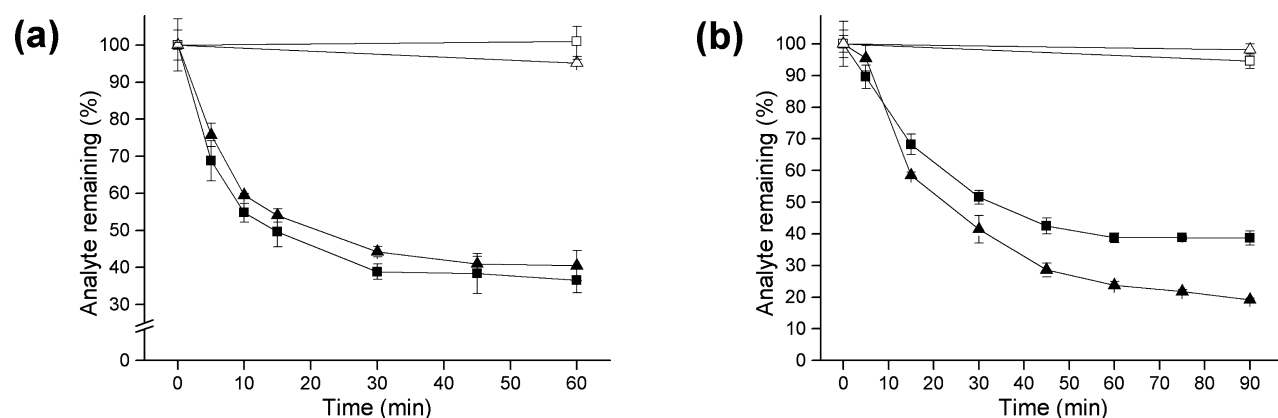


Figure 3. Depletion profile of 1 μM *cis*-ZEN (triangle) and *trans*-ZEN (square) in RLM (a) and HLM (b). The corresponding NADPH-depleted controls clearly show the dependence of phase I metabolism of *cis*-ZEN (blank triangle) and *trans*-ZEN (blank square) on NADPH as cofactor. Error bars represent the standard deviation ($n = 3$ for samples containing NADPH; $n = 2$ for controls).

Table 1. Overview of Compounds, Metabolic Reactions, Retention Times (t_R), Elemental Formulas, Observed Masses, and Errors for *cis*-ZEN Metabolites Formed by RLM or HLM

compd	metabolic reaction	RLM	HLM	t_R	formula	m/z observed	mass error (mDa)
<i>cis</i> -ZEN				15.3	$\text{C}_{18}\text{H}_{21}\text{O}_5$	317.142	+3
M1	+O	×	×	6.5	$\text{C}_{18}\text{H}_{21}\text{O}_6$	333.134	0
M2	+O		×	7.5	$\text{C}_{18}\text{H}_{21}\text{O}_6$	333.134	0
M3	+O	×		8.5	$\text{C}_{18}\text{H}_{21}\text{O}_6$	333.134	0
M4	+O and +2H	×		8.5	$\text{C}_{18}\text{H}_{23}\text{O}_6$	335.151	+1
M5	+O and +2H	×		8.8	$\text{C}_{18}\text{H}_{23}\text{O}_6$	335.151	+1
M6	+O	×	×	10.0	$\text{C}_{18}\text{H}_{21}\text{O}_6$	333.134	0
M7	+O	×	×	10.7	$\text{C}_{18}\text{H}_{21}\text{O}_6$	333.134	0
M8	+O	×	×	10.7	$\text{C}_{18}\text{H}_{21}\text{O}_6$	333.134	0
M9	+2H	×	×	13.1	$\text{C}_{18}\text{H}_{23}\text{O}_5$	319.157	+2
M10	+2H	×	×	13.8	$\text{C}_{18}\text{H}_{23}\text{O}_5$	319.157	+2

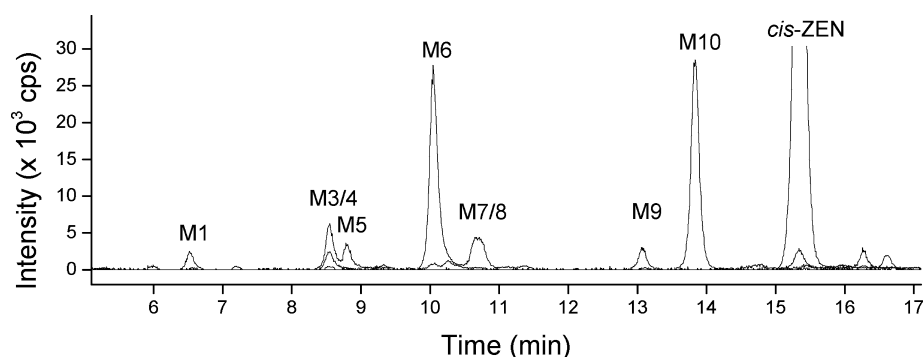


Figure 4. Overlay of extracted ion chromatograms that were obtained by analysis of 10 μM *cis*-ZEN incubated with RLM. The four ion traces, m/z 319.157, m/z 333.134, m/z 335.152, and m/z 317.342, were extracted and combined.

substrate concentration (Figure 3). In the absence of NADPH, *cis*-ZEN levels remain constant. In order to investigate if changes in double bond configuration affect depletion kinetics, the degradation of *cis*-ZEN is displayed in comparison to that of *trans*-ZEN.

Initial degradation constants and half-lives were calculated in approximation to first-order decay functions for RLM and HLM. In RLM, the rate constants for *cis*- and *trans*-ZEN are comparable, with values of 41 ± 3 and $45 \pm 3 \times 10^{-3} \text{ min}^{-1}$, respectively. The half-lives were determined to be 17 ± 1 for *cis*-ZEN and 15 ± 1 for *trans*-ZEN. By contrast, in HLM, *cis*-ZEN is metabolized about 1.4-fold faster than is *trans*-ZEN, with the rate constants being $29 \pm 1 \times 10^{-3} \text{ min}^{-1}$ for *cis*-ZEN

and $20 \pm 1 \times 10^{-3} \text{ min}^{-1}$ for *trans*-ZEN, which is also reflected in their half-lives (24 ± 1 min for *cis*-ZEN and 34 ± 3 min for *trans*-ZEN). A two-sided t -test ($f = 4$, $P = 95\%$) confirmed statistically significant differences for the half-lives of *cis*- and *trans*-ZEN in HLM.

Metabolite Profiles of *cis*-ZEN. Analysis of the RLM and HLM incubations of *cis*-ZEN by high-resolution mass spectrometry (HRMS) revealed a total of 10 unknown metabolites, which are listed in Table 1.

The chromatograms of the metabolite profiles of *cis*-ZEN formed by RLM or HLM, as measured by HRMS, are shown in Figures 4 and 5. Peaks without designation were also observed in controls. All detected metabolites eluted prior to *cis*-ZEN.

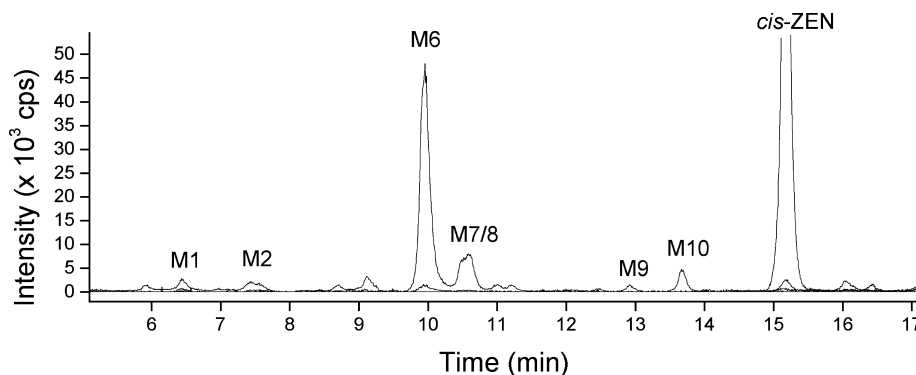


Figure 5. Overlay of extracted ion chromatograms that were obtained by analysis of 10 μM *cis*-ZEN incubated with HLM. The four ion traces, m/z 319.157, m/z 333.134, m/z 335.152, and m/z 317.342, were extracted and combined.

Nine metabolites were detected in RLM incubations (Figure 4). The profile shows two dominating peaks, M6 and M10. The mass of M6 is increased by 15.992 amu, corresponding to a monohydroxylation (+O). Apart from M6, various smaller peaks display the same mass shift, indicating different sites of hydroxylation (M1, M3, M7, and M8). The second main peak, M10, displays a mass shift of +2.015 amu, which suggests a reduction (+2H). The same m/z is observed for the smaller peak, M9. The remaining signals, M4 and M5, are products of sequential reduction and monohydroxylation, with mass shifts of +18.009 amu.

The metabolite pattern of *cis*-ZEN, as catalyzed by HLM, shows seven different metabolites (Figure 5). M6, a monohydroxylated *cis*-ZEN, is the most abundant peak. Several smaller peaks (M1, M2, M7, and M8) also show a m/z corresponding to monohydroxylated *cis*-ZEN, which suggests multiple sites of monohydroxylation. The reductive metabolites M9 and M10 are observed for HLM as well, with both peaks being less pronounced in HLM assays compared those in RLM.

Overall, three different sets of mass increase can be concluded from Table 1: reduction (+2.015 amu, +2H), monohydroxylation (+15.992 amu, +O), and a combination of reduction and monohydroxylation (+18.009 amu, +O and +2 H). The latter is observed only for RLM.

Identification of *cis*-ZEN Metabolites M9 and M10. M9 and M10 share a mass increase of 2.015 amu, which can arise from two metabolic reactions: reduction of the double bond between C11 and C12 or reduction of the ketone. The reduction of the double bond would yield zearalanone, which was excluded by co-chromatography of M9 and M10 with an authentic reference standard. The reduction of the keto group could be confirmed by co-chromatography with synthesized authentic reference standards of α - and β -*cis*-ZEL.

Structure identification of the synthetic *cis*-ZELs was achieved by ^1H nuclear magnetic resonance spectroscopy (NMR) and HRMS. HRMS showed a mass of m/z 319.157 for both α/β -isomers, which matches the calculated exact mass. ^1H NMR allows the configuration of the double bond at C11–C12 to be determined because the vicinal coupling constant between *cis* proton pairs is smaller than the corresponding constant between *trans* proton pairs at chemical double bonds. Thus, the two olefinic protons in α -*trans*-ZEL give rise to a doublet with a vicinal coupling constant of $^3J_{\text{HH,trans}} = 15.4$ Hz. In contrast, α -*cis*-ZEL shows a coupling constant of $^3J_{\text{HH,cis}} = 11.5$ Hz. Likewise, $^3J_{\text{HH,trans}} = 15.6$ Hz for β -*trans*-ZEL decreases to $^3J_{\text{HH,cis}} = 11.5$ Hz in β -*cis*-ZEL. The observed magnitudes of the vicinal ($^3J_{\text{HH}}$) coupling constants are in accordance with the

typical ranges, which are 6–14 Hz for *cis* and 12–18 Hz for *trans* olefinic protons.

DISCUSSION

The present study investigates the quantitative and qualitative phase I metabolism of *cis*-ZEN. Incubations with rat liver microsomes (RLM) or human liver microsomes (HLM) show a depletion of *cis*-ZEN in the presence of NADPH. In the absence of NADPH, *cis*-ZEN is not degraded, implying a strong dependence on NADPH as cofactor for phase I metabolism of *cis*-ZEN. In order to investigate if the isomers differ concerning their depletion kinetics, the degradation of *cis*-ZEN was compared to that of *trans*-ZEN. As a result, depletion characteristics were comparable in RLM, whereas HLM metabolized *cis*-ZEN 1.4-fold faster than *trans*-ZEN. Thus, in HLM, phase I enzymes appear to have a higher affinity toward the *cis* isomer.

The microsomal incubations were subjected to HRMS in order to characterize the resulting metabolites. A multitude of metabolites was generated, as seen from the metabolite patterns (Figures 4 and 5), with vast qualitative similarities in RLM and HLM. Assays using microsomes of both species yield the reduction products α - and β -*cis*-ZEL, as identified by a mass increase of 2.015 amu. α -*cis*-ZEL was found as a main metabolite in RLM. By contrast, α - and β -*cis*-ZEL are only of minor abundance in HLM. Structure identification was conducted by co-chromatography with synthesized authentic standards, which were characterized by HRMS and ^1H NMR. The microsomal transformation of *trans*-ZEN into the reduction products α - and β -*trans*-ZEL has been described in the literature *in vitro* and *in vivo*.^{4–7} α -*trans*-ZEL formation can be regarded as a bioactivation reaction due to a higher binding affinity to the estrogen receptor than its precursor compound *trans*-ZEN. Thus, the estrogenicity of α - and β -*cis*-ZEL should be investigated in the future.

Also, for the formation of monohydroxylated metabolites from *cis*-ZEN, considerable similarities for RLM and HLM are observed. Five isobaric metabolites with a mass shift indicating incorporation of a single oxygen atom are detected for each microsomal species, suggesting multiple reaction targets for the metabolic enzymes of RLM and HLM. The site of hydroxylation cannot be determined due to missing reference compounds. Nevertheless, monohydroxylation can be concluded to be the major phase I metabolic pathway in HLM with respect to metabolite abundance and intensity. This is underpinned by analysis of the same incubation mixtures by HPLC with UV detection (data not shown), which also showed

several monohydroxylated peaks (assigned according to retention time) with similar relative intensities when compared to the HPLC-HRMS chromatograms.

Due to the similarities of monohydroxylated products formed by both microsomal species, RLM might be a potential model for studies of *cis*-ZEN hydroxylation in humans. Regarding *trans*-ZEN, oxidative metabolism was first reported in 2007. Since then, monohydroxylated derivatives of *trans*-ZEN were described repeatedly as metabolites formed by mammalian microsomes including RLM and HLM.^{9–12} A monohydroxylated ZEN derivative was also found in rat urine, demonstrating the presence of oxidative metabolites *in vivo*.¹² It should be the subject of further studies to investigate if differences concerning the positions and stereochemistry of the newly introduced hydroxyl groups exist between *cis*- and *trans*-ZEN.

A difference in RLM and HLM phase I metabolism of *cis*-ZEN can be found in sequential reduction and monhydroxylation. A mass increase of 18.009 amu is seen for two metabolites in RLM but not in HLM. Regarding the *trans* isomer, successive hydroxylation and reduction has been reported for RLM and also for HLM.^{9,11} This finding cannot be attributed to a stereospecific metabolic difference of *cis*- and *trans*-ZEN, as incubations of HLM with *trans*-ZEN did not reveal any +18.009 amu metabolites either (data not shown).

A further question that can be answered from comparison of *cis*- and *trans*-ZEN metabolite profiles is whether *cis*–*trans* isomerization does occur during phase I metabolism. Chromatographic conditions were set up to separate not only *cis*- and *trans*-ZEN but also the *cis* and *trans* isomers of α - and β -ZEL. As a result, it can be stated that incubations of *cis*-ZEN remained free of any *trans*-ZEN or *trans*-ZEL metabolites. Thus, it can be inferred that isomerization does not take place due to isomerases contained within the microsomal preparations or the chosen experimental conditions.

Regarding the enzymes involved, we assume that 3α - and 3β -hydroxysteroid dehydrogenase are involved in the reduction of *cis*-ZEN, as these enzymes are responsible for the reduction of *trans*-ZEN.^{24,25} Human cytochrome P450 (CYP) 1A2 was shown to be highly active in the hydroxylation of *trans*-ZEN.¹¹ Thus, CYP1A2 may also be responsible for hydroxylation of *cis*-ZEN.

In conclusion, this study shows that *cis*-ZEN is extensively metabolized by RLM and HLM. From a qualitative point of view, *cis*-ZEN seems to be transformed following the same metabolic routes as those for *trans*-ZEN. α -*cis*-ZEL is found as a major reductive metabolite of *cis*-ZEN, which might also be a bioactivation process, as seen for α -*trans*-ZEL formation from *trans*-ZEN. Toxicological studies are needed to further investigate if the formed metabolites are more or less potent than *trans*-ZEN in order to protect consumers from unexpected health risks.

AUTHOR INFORMATION

Corresponding Author

*Phone: +49-30-8104-5889. E-mail: sarah.drzymala@bam.de.

Funding

This work was funded by the Federal Institute for Materials Research and Testing.

Notes

The authors declare no competing financial interest.

ACKNOWLEDGMENTS

The authors would like to thank Prof. Dr. Monika Schreiner for the opportunity to use the HRMS facilities at IGZ Großbeeren.

ABBREVIATIONS

HLM, human liver microsomes; HPLC-MS/MS, high-pressure liquid chromatography tandem mass spectrometry; HRMS, high-resolution mass spectrometry; NADPH, nicotinamide adenine dinucleotide phosphate; RLM, rat liver microsomes; ZEL, zearalenol; ZEN, zearalenone

REFERENCES

- (1) EFSA (2011) EFSA panel on contaminants in the food chain. Scientific opinion on the risks for public health related to the presence of zearalenone in food. *EFSA J.* 9:2197, 124.
- (2) FAO (2004) Regulations for Mycotoxins in Food and Feed in 2003. *FAO Food Nutr. Pap.*, 81.
- (3) The Commission of the European Communities (2007) Commission regulation no 1126/2007 amending regulation (EC) no 1881/2006 setting maximum levels for certain contaminants in foodstuffs as regards *Fusarium* toxins in maize and maize products. *Off. J. Eur. Communities: Legis.* 255, 14–17.
- (4) Malekinejad, H., Maas-Bakker, R., and Fink-Gremmels, J. (2006) Species differences in the hepatic biotransformation of zearalenone. *Vet. J.* 172, 96–102.
- (5) Mirocha, C. J., Pathre, S. V., and Robison, T. S. (1981) Comparative metabolism of zearalenone and transmission into bovine milk. *Food Chem. Toxicol.* 19, 25–30.
- (6) Danicke, S., Swiech, E., Buraczewska, L., and Ueberschar, K. H. (2005) Kinetics and metabolism of zearalenone in young female pigs. *J. Anim. Physiol. Anim. Nutr.* 89, 268–276.
- (7) Olsen, M., and Kiessling, K. H. (1983) Species differences in zearalenone-reducing activity in subcellular fractions of liver from female domestic animals. *Acta Pharmacol. Toxicol.* 52, 287–291.
- (8) Shier, W. T., Shier, A. C., Xie, W., and Mirocha, C. J. (2001) Structure–activity relationships for human estrogenic activity in zearalenone mycotoxins. *Toxicol.* 39, 1435–1438.
- (9) Hildebrand, A. A., Pfeiffer, E., Rapp, A., and Metzler, M. (2012) Hydroxylation of the mycotoxin zearalenone at aliphatic positions: novel mammalian metabolites. *Mycotoxin Res.* 28, 1–8.
- (10) Pfeiffer, E., Heyting, A., and Metzler, M. (2007) Novel oxidative metabolites of the mycoestrogen zearalenone *in vitro*. *Mol. Nutr. Food Res.* 51, 867–871.
- (11) Pfeiffer, E., Hildebrand, A., Damm, G., Rapp, A., Cramer, B., Humpf, H. U., and Metzler, M. (2009) Aromatic hydroxylation is a major metabolic pathway of the mycotoxin zearalenone *in vitro*. *Mol. Nutr. Food Res.* 53, 1123–1133.
- (12) Bravin, F., Duca, R. C., Balaguer, P., and Delaforge, M. (2009) *In vitro* cytochrome p450 formation of a mono-hydroxylated metabolite of zearalenone exhibiting estrogenic activities: possible occurrence of this metabolite *in vivo*. *Int. J. Mol. Sci.* 10, 1824–1837.
- (13) Metzler, M., Pfeiffer, E., and Hildebrand, A. (2010) Zearalenone and its metabolites as endocrine disrupting chemicals. *World Mycotoxin J.* 3, 385–401.
- (14) Pfeiffer, E., Kommer, A., Dempe, J. S., Hildebrand, A. A., and Metzler, M. (2011) Absorption and metabolism of the mycotoxin zearalenone and the growth promotor zearanol in Caco-2 cells *in vitro*. *Mol. Nutr. Food Res.* 55, 560–567.
- (15) Warth, B., Sulyok, M., Berthiller, F., Schuhmacher, R., and Krska, R. (2013) New insights into the human metabolism of the *Fusarium* mycotoxins deoxynivalenol and zearalenone. *Toxicol. Lett.* 220, 88–94.
- (16) Richardson, K. E., Hagler, W. M., and Mirocha, C. J. (1985) Production of zearalenone, α - and β -zearalenol, and α - and β -zearalanol by *Fusarium* spp. in rice culture. *J. Agric. Food Chem.* 33, 862–866.

- (17) Munoz, L., Castro, J. L., Cardelle, M., Castedo, L., and Riguera, R. (1989) Acetylated mycotoxins from *Fusarium graminearum*. *Phytochemistry* 28, 83–85.
- (18) Smyth, M. R., and Bernhard Frischkorn, C. G. (1980) Simultaneous determination of the trans and cis forms of zearalenone in cereal products by high-performance liquid chromatography with voltammetric detection. *Anal. Chim. Acta* 115, 293–300.
- (19) Koppen, R., Riedel, J., Proske, M., Drzymala, S., Rasenko, T., Durmaz, V., Weber, M., and Koch, M. (2012) Photochemical trans-/cis-isomerization and quantitation of zearalenone in edible oils. *J. Agric. Food Chem.* 60, 11733–11740.
- (20) Bosch, U., and Mirocha, C. J. (1992) Toxin production by *Fusarium* species from sugar beets and natural occurrence of zearalenone in beets and beet fibers. *Appl. Environ. Microbiol.* 58, 3233–3239.
- (21) Drzymala, S., Riedel, J., Koppen, R., Garbe, L. A., and Koch, M. (2014) Preparation of ¹³C-labelled cis-zearalenone and its application as internal standard in stable isotope dilution analysis. *World Mycotoxin J.* 7, 45–52.
- (22) Obach, R. S. (1999) Prediction of human clearance of twenty-nine drugs from hepatic microsomal intrinsic clearance data: an examination of *in vitro* half-life approach and nonspecific binding to microsomes. *Drug Metab. Dispos.* 27, 1350–1359.
- (23) Smith, W. B., and Watson, W. H. (1987) A conformational investigation of zearalenone and the 6'-zearalenols by carbon and proton NMR spectroscopy. *Magn. Reson. Chem.* 25, 975–980.
- (24) Olsen, M., Pettersson, H., and Kiessling, K. H. (1981) Reduction of zearalenone to zearalenol in female rat liver by 3 alpha-hydroxysteroid dehydrogenase. *Acta Pharmacol. Toxicol.* 48, 157–161.
- (25) Malekinejad, H., Maas-Bakker, R. F., and Fink-Gremmels, J. (2005) Enzyme kinetics of zearalenone biotransformation: pH and cofactor effects. *Arch. Toxicol.* 79, 547–553.